Ann. Zool. Fennici 61: 163–177 ISSN 0003-455X • eISSN 1797-2450
Helsinki 19 November 2024

Dance of the Cave Bear: Honouring the Scientific Legacy of Björn Kurtén

Lack of differences in anatomical structures of the head associated with thermoregulation between Saimaa (*Pusa hispida saimensis*) and Baltic ringed seals (*Pusa hispida botnica*)

Juha Laakkonen[1,*], Heini Nihtilä[1] & Jukka Jernvall[2]

[1] *Division of Veterinary Anatomy and Developmental Biology, Department of Veterinary Biosciences, Faculty of Veterinary Medicine, P.O. Box 66, FI-00014 University of Helsinki, Finland (*corresponding author's e-mail: juha.laakkonen@helsinki.fi)*
[2] *Institute of Biotechnology, P.O. Box 56, FI-00014 University of Helsinki, Finland*

Received 27 Feb. 2024, final version received 10 May 2024, accepted 13 May 2024

Laakkonen, J., Nihtilä, H. & Jernvall, J. 2024: Lack of differences in anatomical structures of the head associated with thermoregulation between Saimaa (*Pusa hispida saimensis*) and Baltic ringed seals (*Pusa hispida botnica*). — *Ann. Zool. Fennici* 61: 163–177.

Prompted by our previous findings of several subtle but distinct differences in some anatomical aspects of the Saimaa (*Pusa hispida saimensis*) and Baltic ringed seals (*Pusa hispida botnica*), particularly in the head region, we investigated the osteological and arterial architecture of the nasal conchae and the ophthalmic rete of through computer tomography, magnetic resonance imaging, arterial silicone injections, dissection, histological examination, and comparison of skull specimens. The conchal and ophthalmic retia, involved in the thermoregulation of mammals, were similar in their anatomical structure to those reported from other pinnipeds and did not differ between the ringed seal subspecies. The endangered status of the Saimaa ringed seal prevented invasive investigation methods helpful for linking anatomical findings to functional properties. However, with silicone models, we were able to confirm the existence of delicate structures such as a separate vibrissal arterial circulation and the lateral and medial posterior ciliary arteries.

Introduction

The endangered Saimaa ringed seal (*Pusa hispida saimensis*) is a subspecies endemic to Lake Saimaa in Finland. In contrast, the Baltic ringed seal (*Pusa hispida botnica*) inhabits the brackish Baltic Sea, which is almost entirely landlocked. Recent research by Löytynoja *et al.* (2023) showed that the Saimaa ringed seal is genetically distinct from other ringed seal subspecies, with an independent evolutionary history that is considerably longer than the formation of Lake Saimaa at the end of the last glaciation. We have previously demonstrated subtle but distinct anatomical differences in the bronchial branching (Laakkonen & Jernvall 2016), temporomandibular joint (Laakkonen & Jernvall 2020), teeth and tongue (Jernvall & Laakkonen unpubl. data) of Saimaa and Baltic ringed seals indicating that these subspecies may be morphologically dis-

Edited by Oscar E. Wilson, University of Helsinki

tinct as well. Because of the noted differences, situated mainly in the head region, we compared the osteological and arterial architecture of the nasal conchae, and the arterial vasculature ophthalmic rete and the mystacial pad of Saimaa and Baltic ringed seals. We aimed to determine whether these subspecies differ in structures of the head related to thermoregulation.

The presence of convoluted sheets of thin turbinate bones in the nasal cavity is a common feature of mammals (Negus 1958, Moore 1981, Hillenius 1992). Traditionally, the turbinates were named after the primary (but not necessarily only) cranial bone attached to them in adult individuals (Moore 1981). However, more recent studies from various mammalian groups revealed a greater complexity of attachments and interrelationships among the nasal regions housing these turbinates (Rowe *et al*. 2005, Smith *et al*. 2007, Macrini 2012, Van Valkenburgh *et al*. 2014a). Van Valkenburgh *et al*. (2011, 2014a) described the bilateral, relatively small nasoturbinates attached to the nasal bones as simple in structure and covered in a combination of sensory and non-sensory epithelia. In carnivores, the nasoturbinates most likely primarily aid in the direction of airflow to the primary olfactory region in the caudal part of the nasal cavity, where blind-ended recesses are formed between olfactory epithelium-covered turbinates attaching to the ethmoidal, frontal, and sphenoid bones (Moore 1981, Craven *et al*. 2007, Van Valkenburgh *et al*. 2011, 2014a, 2014b). The largest sensory area is found on the ethmoturbinates (Van Valkenburgh *et al.* 2011, 2014a). Maxilloturbinates located ventrorostrally to the nasoturbinates in a spatially distinct region are covered by respiratory epithelium and attached to the bilateral maxillary bones. Their anatomical architecture varies considerably between various groups of mammals, from the reduced turbinates of many primates and cetaceans to the usually compact, intricately branched structures of carnivores (Negus 1958, Van Valkenburgh *et al*. 2011, Mason *et al*. 2020).

Murie (1874) reported the convoluted structure of the nasal conchae of seals for the first time almost 150 years ago, and several authors have shown that seals have relatively small olfactory turbinates but branched-type maxilloturbinates with a high surface area (Scott 1954, Negus 1958, Folkow *et al*. 1988, Mills & Christmas 1990). Based on the sectioning of fresh heads, Huntley *et al*. (1984) and, more recently, Lester and Costa (2006) reported large-sized maxilloturbinates from the northern elephant seal (*Mirounga angustirostris)*. Folkow *et al*. (1988) made similar findings from grey seals (*Halichoerus grypus)* and harp seals (*Pagophilus groenlandicus*). Mason *et al.* (2020) recently reported that polar seals have more elaborate maxilloturbinate systems than Mediterranean monk seals (*Monachus monachus*). Descriptions of turbinates of ringed seals are limited. However, based on computed tomography of the Baikal seal (*Pusa sibirica*), Endo *et al.* (1999) reported that they correspond to the intricately branched type known from many carnivores (Negus 1958, Moore 1981, Craven *et al*. 2007, Van Valkenburgh *et al*. 2011, 2014a, 2014b, Mason *et al*. 2020). Based on a magnetic resonance imaging study covering all body regions of one Saimaa ringed seal specimen, Usenius *et al*. (2007) described the maxilloturbinates of Saimaa ringed seals as folded structures. In addition, Hyvärinen and Nieminen (1990), Amano *et al*. (2002), and Laakkonen and Jernvall (2020) found differences in the skull bone proportions of ringed seals. However, none of these differences were explicitly related to the nasal region.

As for the function of nasal conchae, Hillenius (1992) suggested the reduction of respiratory water loss to be an important adaptation to the high ventilation rates typical for mammals, as it allows them to conserve two-thirds of the humidity of the exhaled air (Walker & Wells 1961, Jackson & Schmidt-Nielsen 1964, Hillenius & Ruben 2004, Hillenius 1992). More recently, Owerkowicz *et al*. (2015) hypothesised that maxilloturbinates were initially selected for heat dissipation and brain cooling and later evolved for heat and moisture conservation (*see* also Crompton *et al*. 2017). In early studies, Scholander *et al*. (1950) and Irving and Hart (1957) showed that the metabolic economy of the seals in cold water was preserved by efficient cooling of all body surfaces and later studies noted the role of respiratory turbinates in heat and water loss reduction also in pinnipeds (Boyd 1975, Ortiz *et al*. 1978, Huntley *et al*. 1984, Folkow & Blix 1987, Mason *et al*. 2020, Flekkøy *et al*. 2023, Cheon *et al*. 2023).

In addition to the large nasal and infraorbital area housing the system of turbinates (Jones *et al*. 2015, Milne *et al*. 2022), pinniped eyes are large, both relatively and absolutely, and in most species the orbit size is positively correlated with diving depth (Debey & Pyenson 2013). Tandler (1899) reported the presence of an ophthalmic rete in pinnipeds over 120 years ago. The richness of the eye vascularization (Ninomiya *et al*. 2014) and its arrangement suggest that countercurrent heat exchange may occur in the ophthalmic region (Folkow *et al*. 1988). Sufficient heat in the deeper layers of the eye may be necessary not only for the function of photoreceptors but for a flow-dampening effect by maintaining resistance to blood flow in the orbit, along with fat fluidity enabling smooth eyeball movement (Ninomiya & Yoshida 2007) while the surface layer of the eye (cornea) remains cooler to prevent heat loss.

Because Dehnhart *et al*. (1998) revealed with a thermographic examination of the mystical and supraorbital vibrissal pads to be areas of excessive heat loss in harbour seals (*Phoca vitulina*), and Erdsack *et al*. (2014) showed differences between seal species in the thermoregulation of the vibrissae, the vasculature of the mystacial pad was of interest to us as a third head area related to thermoregulation. The thermally clearly defined areas against the rest of the head suggest the existence of a separate vibrissal blood circulation (Dehnhart *et al*. 1998). In addition, several authors have reported the pinniped vibrissal follicle-sinus complexes to be generously supplied via blood sinuses (Ling 1977, Hyvärinen 1989, Hyvärinen & Katajisto 1984). Finally, Käkelä and Hyvärinen (1993) showed in Saimaa ringed seals that the thick subcutaneous fat tissue layer (known as blubber) has a specific fatty acid composition and density in the vibrissal pad areas that differ from those of other body regions.

We used silicone models to determine the arterial circulation of the areas relevant to this study. We complemented these models with an osteological examination of museum specimens and histological slides, dissection of Saimaa and Baltic ringed seal carcasses, and magnetic resonance imaging and computer tomography of the head regions. This paper is part of our comprehensive studies on the comparative anatomy of ringed seals to improve our understanding of the evolutionary phenomics of mammals.

Material and methods

All Saimaa ringed seals found dead are collected and assigned a specimen number by the staff of Parks and Wildlife Finland, a unit of the state institution Metsähallitus, and stored at –20 °C until necropsy at the facilities of the Finnish Food Authority pathology unit in Oulu, Finland, where various samples are collected for research and conservation purposes. Specimens are usually in various stages of decomposition. However, 12 seals collected between 2017 and 2021 were in relatively good condition (Tables 1 and 2), enabling partial anatomical examination or collection of selected anatomical samples during the necropsies in Oulu. Upon recovery, the animals had been dead anywhere from a few to more than 24 hours. The carcasses were stored frozen until necropsy. Four individuals chosen for more detailed anatomical examination were shipped frozen directly from the Metsähallitus storage facility to the dissection facility of the Veterinary Faculty of the University of Helsinki in Helsinki. Based on a research agreement, Metsähallitus permitted the University of Helsinki to use the Saimaa ringed seal material in research. We could examine some individuals only for limited aspects of this study due to damage to one side of the head or the poor condition of the targeted anatomical structure (the eyes) upon recovery. The eyes of four Saimaa ringed seal individuals that had retained their shape relatively intact until necropsy (Table 2) were measured with a digital sliding calliper upon removal from the orbit. The eyes of one Saimaa and one Baltic ringed seal individual were measured with imaging techniques (*see* below; Table 2). All examined seals were found dead in water or on the ice, or they were by-catch found in gill nets.

Additionally, three Baltic ringed seals (Table 1) were legally shot by a hunter in the Bothnian Bay (the northernmost part of the brackish Baltic Sea). They were shipped frozen to the Veterinary Faculty of the University of Helsinki for anatomical examination. Baltic ringed seals are legally hunted in Finland, and the studied individuals were shot for reasons unrelated to our research. The examined seals were age-grouped according to body weight: under 30-kg individuals were pups, 30–42-kg individuals were subadults, and over 42-kg were adults. Anatomical terminology was in accordance with the International Committee on Veterinary Gross Anatomical Nomenclature (2017).

Computer tomography scan protocol

All specimens were thawed before imaging, which aimed to obtain as much anatomical data as possible from structures unrelated to this study. Non-contrast entire-body helical CT imaging was performed for four individuals (Table 1) with the GE LightSpeed VCT 64 scanner (GE Healthcare, Fairfield, Connecticut, USA) at the Veterinary Teaching Hospital of the University of Helsinki. All specimens were scanned with the ventral side down from the nose's tip to the

Table 1. Saimaa and Baltic ringed seals examined with magnetic resonance imaging (MRI) or a computed tomography scanner (CT) and/or treated with silicone injections for visualising the ophthalmic and nasal arterial arrangement (in one or both sides of the skull). Metsähallitus and Natural Resources Institute Finland (Luke) specimens are indicated with one and two asterisks, respectively.

Subspecies	Specimen number	Sex	Weight (kg)	CT or MRI	Silicone casts
Saimaa ringed seal	2670*	female	42	CT	–
Saimaa ringed seal	2698*	male	38	CT	both sides
Saimaa ringed seal	2704*	female	35	MRI	both sides
Saimaa ringed seal	2726*	male	16	–	both sides
Saimaa ringed seal	2742*	female	16	–	both sides
Saimaa ringed seal	2744*	female	19	–	both sides
Saimaa ringed seal	2745*	female	17	–	both sides
Saimaa ringed seal	2747*	female	17	MRI	left side
Baltic ringed seal	458**	female	23	CT	right side
Baltic ringed seal	459**	female	46	CT	–
Baltic ringed seal	668**	female	53	–	both sides

Table 2. Saimaa and Baltic ringed seal specimens used in the histological examination of eye structure. The size of the removed eyeball was measured from some individuals during the cadaver dissection. The eyes of specimens 2704 and 459 were measured using MRI or CT. HE = hematoxylin and eosin; Metsähallitus and Natural Resources Institute Finland (Luke) specimens are indicated with one and two asterisks, respectively.

Subspecies	Specimen number	Sex	Weight (kg)	Lateromedial width (mm) left eye/right eye	Rostrocaudal width (mm) left eye/right eye	Histology
Saimaa ringed seal	2670*	female	42	–	–	HE
Saimaa ringed seal	2698*	male	38	–	–	HE
Saimaa ringed seal	2704*	female	35	38.0/42.0	36.0/40.0	HE
Saimaa ringed seal	2726*	male	16	–	–	HE
Saimaa ringed seal	2744*	female	19	–	–	HE
Saimaa ringed seal	2745*	female	17	–	–	HE
Saimaa ringed seal	2747*	female	17	–	–	HE
Saimaa ringed seal	2756*	male	50	43.4/46.6	42.5/42.5	HE + Masson
Saimaa ringed seal	2778*	female	23	36.6/30.6	33.9/35.4	HE + Masson
Saimaa ringed seal	2782*	female	22	34.5/33.8	36.3/38.0	HE + Masson
Saimaa ringed seal	2806*	male	20	33.7/35.8	35.6/35.2	HE + Masson
Baltic ringed seal	459**	female	46	41.0/40.0	42.0/38.0	HE

tail's tip. The scanning parameters were 100 kV, 750 mAs, interval 0.625 mm, slice thickness 0.625 mm. The bone algorithm's centre point and window width were 500 and 3500 Hounsfield units (HU), respectively. For viewing in the soft tissue window, the centre point was 40, and the width was 400 HU. The matrix size was 512 × 512 (pixels). All image analyses were performed with an Imaios DICOM viewer.

Magnetic resonance imaging protocol

All imaged specimens were thawed before imaging, which aimed to obtain more detailed information on soft tissues than possible with CT. Magnetic resonance imaging (MRI) of the head and torso in the sagittal and transverse planes was performed for two Saimaa ringed seals at the Veterinary Teaching Hospital of the University of Helsinki using a 1.5 Tesla scanner (Philips, Ingenia 1.5T S, Philips Medical System). Imaging parameters designed for imaging living tissues (of veterinary hospital patients) had to be adjusted to account for the thick blubber layer of ringed seals. The carcass was imaged while lying on its back, and a head coil was used for the head region. The protocol and parameters for imaging were: Turbo-Spin-Echo T2-weighted and T1-weighted dorsal, sagittal, and transversal plane MRI; T2: Imaging parameters for sagittal imaging TR 13 123 ms; TE 110 ms, TR for transversal imaging 12 788 ms; TE 110 ms, for dorsal imaging TR 100 ms; TE 4040 ms, flip angle 90°, slice thickness 2.5 mm; T1: Imaging parameters for sagittal, transversal, and dorsal imaging TR 633 ms; TE 15 ms, flip angle 90°, slice thickness 2.5 mm. All image analyses were performed with an Imaios DICOM viewer. Magnetic imaging was not feasible for the hunted Baltic ringed seal specimens because of the bullet fragments in their bodies. Once the CT and MRI imaging were completed, silicone casts of the selected specimens were produced of the head region arteries (*see* below for the method) (Table 1). The silicone-injected cranial arteries of one Saimaa ringed seal (Metsähallitus specimen 2704) were visualised with an additional MRI head series with black blood flip angle 10°, TE 34 ms, TR 24 ms, and slice thickness 1.5 mm. Due to the small number of specimens available and damage in the head area in some specimens, we did not quantify or provide statistics on the imaging data.

Arterial silicone models

Silicone casts of the arterial arrangement of the head region of seven Saimaa ringed seal and two Baltic ringed seal carcasses (Table 1) were created by injecting (without rinsing or perfusion pressure measurements) silicone (3M Express$^{\text{TM}}$ 2 Light Body Standard Quick and 3M Express$^{\text{TM}}$ 2, Light Body Flow Quick) into the external carotid artery, as described in detail by Laakkonen and Kivalo (2013). The silicone was applied as long as it easily flowed into the arteries and stopped as soon as any resistance in the flow was met. After allowing at least ten minutes for the silicone to set, the heads of the injected carcasses were removed and all soft tissue macerated with either a chemical (14% sodium hypochlorite solution, Sigma-Aldric, Switzerland) or an enzyme (papain, 5 g l^{-1}, Bauer Handels, Switzerland) maceration process, as described by Laakkonen and Kivalo (2013) and Granroth and Laakkonen (2023). The diameters of the selected arteries in the casts were measured with a digital sliding calliper (Digitronic calliper, Polycal series, Moore & Wright). Complete and reliable casts of the venous circulation were unsuccessful due to the valves blocking silicone flow. Because of our need to obtain replicate casts to discern any individual variation and the low number of adequately preserved Saimaa ringed seal individuals available, the use of other resin types was not feasible.

Additional material examined

The following additional osteological skull material at the osteological collections of the Finnish Museum of Natural History in Helsinki, Finland (MZH) was examined for comparative purposes: *Pusa hispida saimensis* MZH 112, MZH 2293, MZH 6289, MZH 6462, MZH 5689, MZH 5703, MZH 5704, MZH 6462, MZH 6728; *Pusa hispida botnica* MZH 2279, MZH 2113, MZH 47345, MZH 49879.

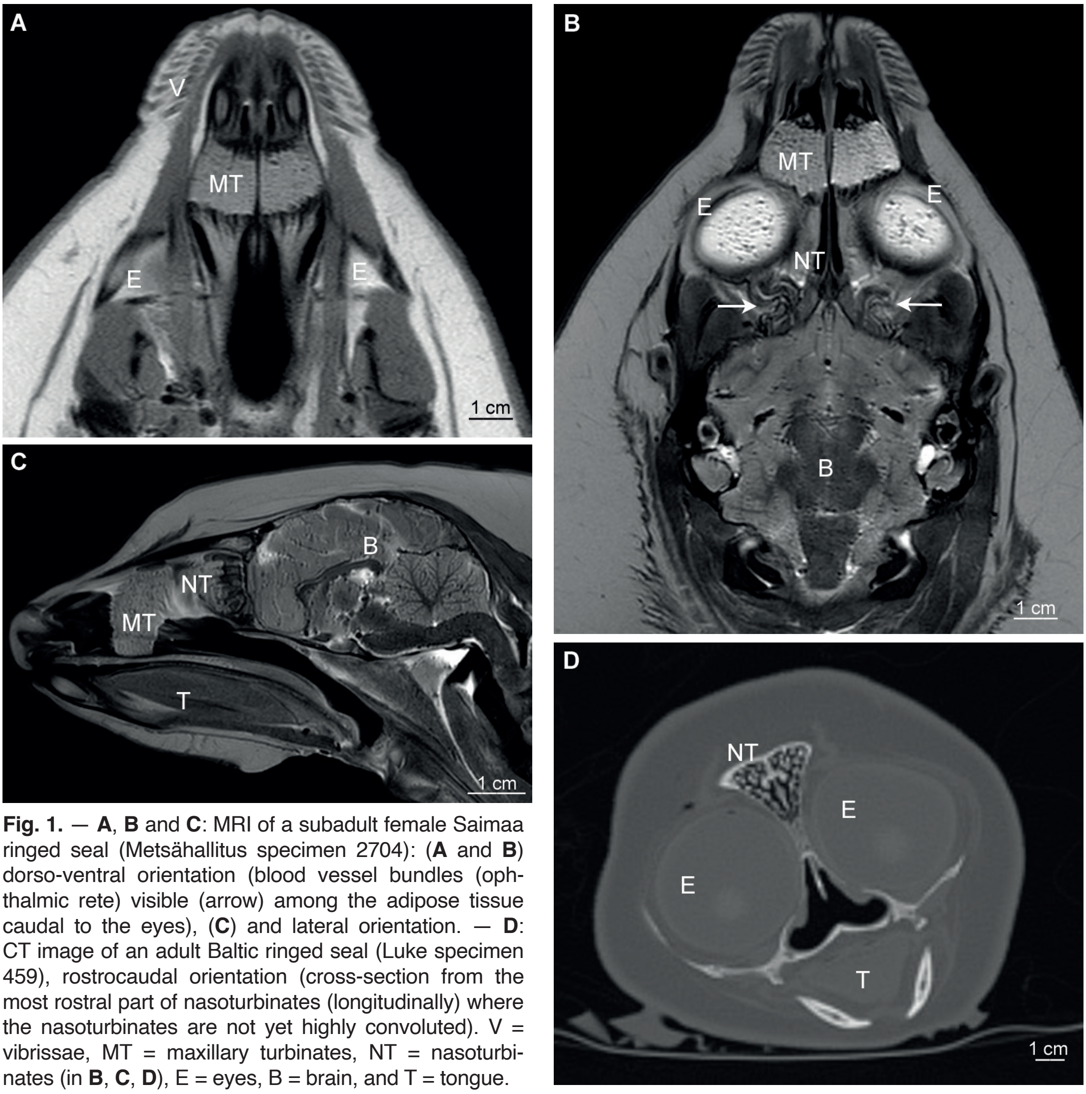

Fig. 1. — **A**, **B** and **C**: MRI of a subadult female Saimaa ringed seal (Metsähallitus specimen 2704): (**A** and **B**) dorso-ventral orientation (blood vessel bundles (ophthalmic rete) visible (arrow) among the adipose tissue caudal to the eyes), (**C**) and lateral orientation. — **D**: CT image of an adult Baltic ringed seal (Luke specimen 459), rostrocaudal orientation (cross-section from the most rostral part of nasoturbinates (longitudinally) where the nasoturbinates are not yet highly convoluted). V = vibrissae, MT = maxillary turbinates, NT = nasoturbinates (in **B**, **C**, **D**), E = eyes, B = brain, and T = tongue.

Histological procedure

We prepared standard histological samples of the eyes of 10 Saimaa ringed seals and one Baltic ringed seal (Table 2) and stained them using hematoxylin and eosin (HE) for light microscope examination. Eyes from four Saimaa ringed seal individuals were examined in more detail by adding Masson's trichrome stain (used to visualise connective tissues) to the histological examination protocol. Representative slides were scanned (BI histoscanner, Institute of Biotechnology, Histoscanner, University of Helsinki, Finland) for illustrative purposes. The scanner uses a 4-MP CMOS camera with 130 fps speed. It has a 0.24 um/pixel resolution with the combined 20X/0.8 NA objective (equivalent to 40× magnification).

Results

The blubber layer of the head region was considerably thinner than the layer around the torso in both the Saimaa and Baltic ringed seals (Fig. 1A–C). Due to the large size of the orbits (Figs. 2, 3 and Table 2), the nasal cavity became increasingly narrow towards the caudal direc-

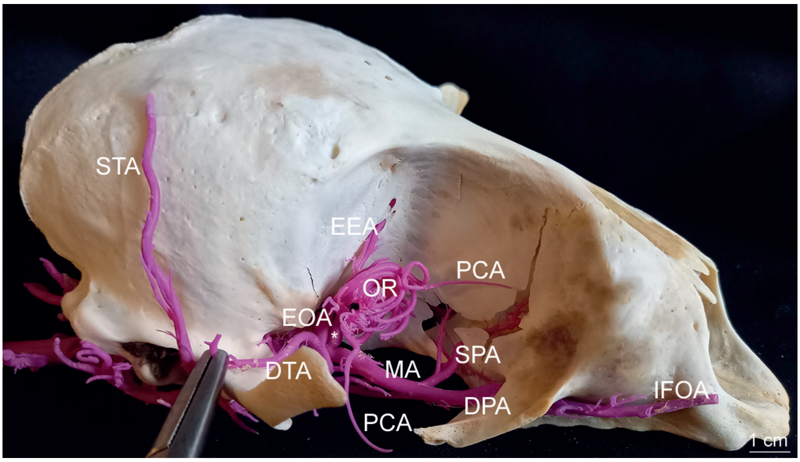

Fig. 2. Dorsolateral view of the right side of the skull of a Baltic ringed seal (Luke specimen 668) showing the extracranially located ophthalmic rete in the orbit (OR). MA = maxillary artery, STA = superficial temporal artery, DTA = deep temporal artery (moved to the lateral direction with forceps to show the external ophthalmic artery (EOA) and a branch connecting to the internal ophthalmic artery (asterisk)), EA = external ethmoidal artery, PCA = posterior ciliary artery, DPA = descending palatine artery, SPA = sphenopalatine artery, IFOA = infraorbital artery.

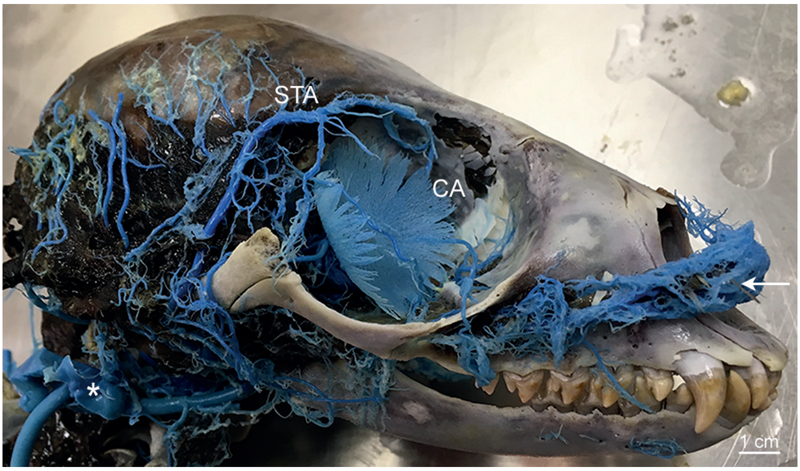

Fig. 3. Skull of a Saimaa ringed seal (Metsähallitus specimen 2726) lateral view, photographed during the chemical maceration process. Some leakage of silicone occurred in the pharyngeal area (asterisk). The arteries entering into the vibrassal pad (arrow) were so numerous that they bundled together when all the soft tissue was macerated from this region (the branches were visible separately when the specimen was kept in water). STA = superficial temporal artery, CA = choroidal arteries.

tion, and, in all specimens, the interorbital separation was under 10 mm, leaving little space for the frontal sinus. The maxilloturbinates did not reach the anterior nasal aperture (Fig. 4) in either subspecies. Viewing from this rostral nasal opening (Fig. 4), the branched-type maxilloturbinates almost fully occupied the nasal cavity space in dorsoventral orientation, and their maximum height and width exceeded those of nasal aperture. A narrow space separates the bilateral maxilloturbinates from the nasal cavity's median plate (*septum nasi*). However, no open passage was found on the ventral side through the nasal cavity to the nasopharynx. At the rostral end of the maxilloturbinates, two cartilaginous extensions (ridges) from the lateral wall of the nasal cavity attached to the dorsal and the middle maxilloturbinate masses, respectively

Fig. 4. Nasal cavity and maxilloturbinates of an adult Saimaa ringed seal (Metsähallitus specimen 2704) in medio-rostral orientation of the right side of the nasal cavity. The attachment ridges of the dorsal and medial maxilloturbibate mass to the lateral wall of the nasal cavity are indicated with arrows.

(Fig. 4). The maxilloturbinates attached dorsally to the incisive, nasal, and maxillary bones. As the ridges shortened towards the caudal direction, they appeared to divide, providing multiple attachments for the maxilloturbinates to the lateral cavity wall (Fig. 1D). The maxilloturbinate mass consisted of three separate parts corresponding to the *concha nasalis dorsalis* and *media*, and the *os conchae nasalis ventralis*. The orientation of the maxilloturbinate mass differed slightly between specimens, but especially the ventral part of the maxilloturbinate mass was slightly dorsally oriented towards the nasal aperture (Fig. 4).

In cross-section, the maxilloturbinates of both the Saimaa and Baltic ringed seals consisted of compact, intricately branched bilateral bony structures (Fig. 4). The airspace between the conchal lamellae (without any soft tissue) was less than 0.5 mm (Fig. 4). Only a small part of the turbinate mass attached dorsally to the narrow nasal bones. The narrow passage consisted of only a few bony sheets guiding air to the region of the frontal bones, where the ethmoturbinate mass widened in the caudal direction as it attached to the ethmoid bone (Fig. 1D).

At the branching of the superficial temporal artery, the maxillary artery first gave off several arteries to the mandibular region before, at the laterocaudal corner of the orbit, giving rise to the external ophthalmic artery and a branch (*ramus anatomicus cum arteria ophthalmica interna*) joining the internal ophthalmic artery. At this same region, the deep temporal artery branched from the lateral side of the maxillary artery to ascend in the dorsal direction (Fig. 2). The diameter of the external ophthalmic artery was 2–3 mm in adult Saimaa and Baltic ringed seals (Metsähallitus specimens 2698, 2704 and Luke specimen 668) before branching into the lacrimal, supraorbital, and internal ophthalmic arteries (not shown). The external ophthalmic artery gave rise to the external ethmoidal artery that penetrated the ethmoidal foramen (Fig. 2). After entering the cranium, the external ethmoidal artery continued through the *lamina cribrosa* to branch and supply the ethmoturbinate mass (not shown). Many of these small vessels continued to reach the maxilloturbinates (Fig. 5). The branch of the maxillary artery joining the internal ophthalmic artery rose just rostral from the origin of the external ophthalmic artery and was approximately 2 mm in diameter in the adult specimens. Together with the external ophthalmic artery, it supplied several orbital and bulbar structures, demonstrating minor variations in the branching pattern of these vessels. The external ophthalmic artery branched into many smaller entwining vessels (diameters ranging from 960 to 1280 µm in adult specimens), which, together with the branches of the internal ophthalmic artery, formed a bundle, i.e., the ophthalmic rete (Fig. 2). The retinal and choroidal arteries derived from this rete. The choroidal arteries formed a calyx-like structure covering the entire caudal part of the eye (Figs. 3 and 6). Of other branches of the ophthalmic artery, the lateral and medial posterior ciliary arteries, supplying the structures of the anterior part of the eye, were visible in the silicone casts (Figs. 2 and 6). They originated from the external ophthalmic artery.

Fig. 5. Medial view of the right side nasal cavity showing the mucosal rete (MR) of the maxilloturbinates of a Saimaa ringed seal (Metsähallitus specimen 2744). MA = maxillary artery, PCA = posterior ciliary artery, DPA = descending palatine artery.

The eyes of both subspecies were large but only the eyes of one Baltic ringed seal were measured due to the shooting damage inflicted on the other Baltic ringed seal skulls (Table 2).

After supplying the eye, the maxillary artery gave medially off the descending palatine artery (Fig. 2), which, at the caudal edge of the hard palate, gave rostrally off the major palatine artery and caudally off the minor palatine artery. After this, the descending palatine artery sent a branch, i.e., the sphenopalatine artery, to pass through the sizeable sphenopalatine foramen to form a longitudinally oriented conchal mucosal rete supplying the mucosal rete of the maxilloturbinates (Fig. 5). The maxillary artery continued to the rostral region by ascending to pass through the maxillary canal (Fig. 2). Upon emerging from the intraorbital foramen, the similarly named artery continued forward to the nasal region, where it supplied the vibrissae around the mouth, among others (Fig. 3). The branches leading to the mystical pad area were so numerous that the bundled together when the model was cleared of any soft tissue.

The histological examination provided a microscopic view of the structure of the ophthalmic rete of the Saimaa and Baltic ringed seals visualised macroscopically by the silicone casts and confirmed that it was embedded in adipose tissue covering the caudal side of the eyeball (Fig. 7).

Discussion

Our previous comparative analyses on the anatomy of Saimaa and Baltic ringed seals revealed subtle but distinct differences in several (Laakkonen & Jernvall 2016, Laakkonen & Jernvall 2020, Jernvall & Laakkonen unpubl. data) but not in all anatomical apparatus (Laakkonen & Nihtilä 2021, Laakkonen 2021, Laakkonen & Vedrines 2022, Laakkonen *et al.* 2024) indicating that the morphologically separating features are not associated with any particular anatomical apparatus or organ system. Furthermore, while the upper respiratory tract of the Saimaa ringed seal closely resembled that of the Baltic ringed seal (*see* above), differences were detected earlier in the lower respiratory tract (Laakkonen & Jernvall 2016), demonstrating regional variation within an anatomical apparatus between the subspecies.

Fig. 6. The lateral and medial posterior ciliary arteries (arrows) ending in a comb-like branching pattern (turned upwards by forceps for better visualisation (Metsähallitus specimen 2726). O = orbit, CA = choroidal arteries.

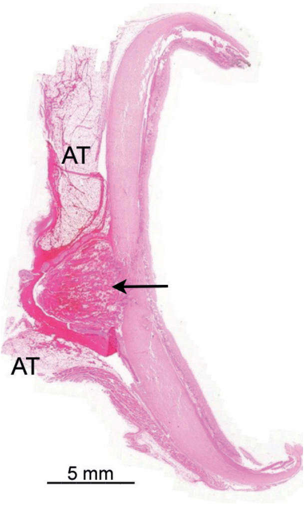

Fig. 7. Histological section (HE stain) of Saimaa ringed seal eye (caudal side to the left) showing the choroidoretinal arteries that form an arterial network (arrow) around the optic nerve (not visible in this layer) at the posterior pole of the eyeball (Metsähallitus specimen 2745). AT = adipose tissue.

Our finding that the anatomy of the nasal conchae of Saimaa ringed seals corresponds to that of the Baltic ringed seal is in line with previous comparative analysis of mammals (Negus 1958, Van Valkenburgh *et al*. 2011, Mason *et al*. 2020). As reported by Folkow *et al*. (1988) for grey and harp seals, the extension of the nasal conchae was short in Saimaa and Baltic ringed seals (Figs. 1 and 4), and the maxilloturbinate masses were of a similar shape to those reported from other seals (Mason *et al.* 2020). Among mammals, the regional morphology of the maxilloturbinates varies with skull shape. In some species, the maxilloturbinates are ventrally positioned in the nasal passage while extending to the nasal roof in other species (Martinez *et al.* 2023). Unlike in horses and some other mammal species (Martinez *et al*. 2023, Simoens *et al*. 1996), no unobstructed passage (to nasopharynx) on the ventral side of the nasal cavity was found in ringed seals (Figs. 1C and 4). The anteroposterior location of the maxilloturbinates also varies considerably between mammal species (Martinez *et al*. 2023). The variation in the orientation of the maxilloturbinate mass between the ringed seal specimens of our study was likely due to age differences, as we observed a more prominent dorsal orientation towards the nasal aperture in young individuals.

Variations occur among mammal species in the configuration and complexity of the maxilloturbinates, but these variations seem to be correlated with phylogenetic groups rather than with the environment (Negus 1958, Hillenius 1992, Moore 1981, Green *et al.* 2012, Martinez *et al.* 2023). Mason *et al*. (2020) reported that within pinnipeds, the maxilloturbinates surface areas are higher in polar seals than in monk seals. We could not assess the possible effect of latitude on the surface area of maxilloturbinates in Saimaa and Baltic ringed seals because we did not measure these. Furthermore, these subspecies partly overlap in latitudinal distribution. However, they share with terrestrial carnivores and other pinnipeds the compact, intricately branched maxilloturbinates that display a dendritic pattern in cross-section (Negus 1958, Endo *et al.* 1999, Usenius *et al*. 2007, Mason *et al*. 2020; Fig. 1).

The roots of the maxilloturbinates from the lateral wall were visible in the bone specimens of our study (Fig. 4) and in the tomogram sections (Fig. 1D). Mason *et al.* (2020) reported a similar anatomical arrangement from other phocid species. However, the number of roots differed between species (Mason *et al.* 2020). In Saimaa and Baltic ringed seals, the number of bone ridges connecting the maxilloturbinates to the latero-caudal part of the nasal cavity appeared to be three at least. However, they were difficult to visualise, especially in the Baltic ringed seal specimens, due to damage caused by shot wounds.

In mammals, the short distance from the centre of the airstream to the nearest mucosal surface of the maxilloturbinates (less than 0.5 mm) facilitates heat and water exchange between the airstream and the mucosa of the concha (Jackson & Schmidt-Nielsen 1964, Schmidt-Nielsen *et al.* 1970). Based on the microscopical examination, Folkow *et al*. (1988) reported that the capillary connections between the retial arteries and veins in the nasal mucosa of grey and harp seals were abundant along the length of the rete. However, a moderate number of arterio-venous anastomoses were present only in the rostral region of the rete. Furthermore, the venous supply of the conchal rete was much greater than the arterial supply (Folkow *et al.* 1988). As the conchal arterial supply of the Saimaa and Baltic ringed seals (Fig. 5) was similar to that of grey and harp seals (Folkow *et al*. 1988), it is likely that ringed seals also possess extensive venous vasculature in their conchal rete.

Because of the multiple functional demands placed on the cranium (vision, feeding, conditioning of incoming air, and olfaction), having both greatly expanded olfactory and respiratory turbinates may not be possible (Van Valkenburgh *et al.* 2011). Repenning (1976) argued that a reduction in olfactory turbinates in pinnipeds is associated with the greatly enlarged orbits in extant and extinct species. Endo *et al*. (1999) suggested that the enlarged orbit of the Baikal seal (*Pusa sibirica*) may have influenced the form and function of the masticatory and respiratory systems of this subspecies, leading to an arrangement where the caudal part of the nasal cavity and nasopharynx are compacted ventrally. This arrangement leaves little space for the frontal sinus, as the interorbital separation is thin (Endo *et al*. 1999; Figs. 1D and 2). The frontal sinus function is poorly understood (Curtis & Van Valkenburgh 2014). It may serve a minimal function and develop in areas of the skull where the bone is biomechanically unnecessary (Witmer 1997), or by altering the skull shape, it may act in the absorption of shock or dissipation of stress in feeding or combat situations (Curtis & Van Valkenburgh 2014). The frontal sinus is lined with mucosal epithelium and maintains direct or indirect communication with the nasal cavity via a small opening (*ostium*). At least in some species, the mucus from the frontal sinus drains into the nasal cavity (Dolezal & Baker 1983), helping to prevent the drying of the nasal airways. As ringed seals are unlikely to have use for any of the suggested functions, they have little need for a large frontal sinus. The shift from a terrestrial to an aquatic existence selects for several physiological and morphological adaptations that relate, for example, to increasing and variable atmospheric pressure (Curtis *et al*. 2014). In shallow divers, the changes in skull shape resulting in a small frontal sinus may provide room for enlarged eyes (Curtis *et al*. 2014).

Pinniped eyes, in particular, are large, in both absolute and relative terms (Jamieson & Fisher 1972, Welsch *et al.* 2001, Mass & Supin 2007, Debey & Pyenson 2013, Smodlaka *et al.* 2016; Table 2). The prominent vasculature and anatomical position of the ophthalmic rete protected by the adipose tissue suggest that countercurrent heat exchange may take place in the orbital area of pinnipeds and cetaceans (Folkow *et al*. 1988, Ninomiya *et al*. 2014; Fig. 7).

Based on the silicone casts, we have previously documented the branching pattern of the external carotid artery until its division into the superficial temporal and maxillary arteries, and the intracranial arterial arrangement in Saimaa and the Baltic ringed seals (Laakkonen *et al*. 2024). In this study, we documented that the main suppliers of the ocular and nasal regions in these seals, originating from the maxillary artery after branching of the superficial temporal artery, closely resembled the arrangement reported from other pinnipeds (Boyd 1975, Folkow *et al.* 1988) and terrestrial mammal species (Negus 1958, Carlton & McKean 1977, Simoens *et al.* 1996).

The bilaterally symmetrical ophthalmic and conchal retia visualised by various corrosion techniques are characteristic of the vessel arrangement of these regions (Folkow *et al*. 1988, Simoens *et al.* 1996, Ninomiya & Yoshida 2007, Ninomiya *et al*. 2014, and this study). In both subspecies of our study, the ophthalmic rete consisted of several entwining arteries located extracranially in the orbital fossa embedded in insulating adipose tissue, as previously reported for other pinniped and cetacean species (Tandler 1899, Folkow *et al*. 1988, Ninomiya *et al*. 2014; Figs. 1B and 2). While the eye was supplied via the external ophthalmic artery in pinnipeds, including the Saimaa and Baltic ringed seals, the basilar rete via the spinal rete was the primary blood supply source to the rete in dolphins (Ninomiya *et al*. 2014). The ophthalmic rete of spotted seals (*Phoca largha*), described by Ninomiya *et al.* (2014), was very similar to what we documented in Saimaa and Baltic ringed seals (Fig. 2). However, the rete in the California sea lion (*Zalophus californicus*) was considerably smaller and less complex (Ninomiya *et al.* 2014).

The diameter of the external ophthalmic artery (2–3 mm) in adult Saimaa and Baltic ringed seals was similar to that (1.8 mm) reported for the spotted seal, but the vessels forming the ophthalmic rete were considerably more prominent in the ringed seals (960–1280 µm) than those in the spotted seal (300–350 µm; Ninomiya *et al*. 2014). However, the arterial measurements did not necessarily reflect the actual size of the vessel, as the arteries may expand depending on the pressure applied during the injection process, and the diameter may depend on the size and age of the animal (not reported for the spotted seal in Ninomiya *et al*. 2014). The ophthalmic artery diameter in the California sea lion is approximately 1.3 mm, similar to that reported from the horse (1.4 mm), whose eye contains approximately the same volume as that of the sea lion (Ninomiya *et al*. 2014). Ninomiya *et al*. (2014) concluded that the ophthalmic artery of the California sea lion can therefore transport nearly three times as much blood into the eye as that of the horse. Simoens *et al*. (1996) reported that variations in the origin and ramification pattern of the retrobulbar arteries were numerous in the horse. Similarly, we observed variation in the number of orbital branches of the external ophthalmic artery in both Saimaa and Baltic ringed seals.

The silicone casts helped to demonstrate even delicate blood vessel structures, such as the lateral and medial posterior ciliary arteries (Fig. 6). Previously we have shown with this method the tiny arterial circle around the upper pituitary stalk (Laakkonen *et al*. 2024). However, the low number of specimens available in this study prevented any quantitative analyses on the arterial size differences of the ophthalmic region. The venous valves prevented the preparation of complete venous casts, a complication reported previously in the casts of various mammals (Carlton & McKean 1977, Folkow *et al*. 1988).

Compared to other Carnivora species, pinnipeds have significantly larger infraorbital foramen areas housing fewer but longer and more innervated vibrissae (Milne *et al*. 2022). With the use of silicone casts, we were able to confirm that in both ringed seal subspecies, the infraorbital artery branched widely to the mystacial pad to supply each vibrissae separately (Fig. 3). This arrangement supports the previous suggestion based on thermographic examination (Dehnhart *et al*. 1998) that a separate vibrissal blood circulation exists in seals.

The trunk of Saimaa ringed seals is typically covered with a 4–5 cm thick layer of blubber that may form 43% of the body mass (Auttila *et al.* 2016). At the orbital and nasal regions, the blubber layer can be half as thin (Endo *et al.* 1999, Usenius *et al*. 2007; Fig. 1A–C), but this does not necessarily create a potential heat loss area because the blubber is distributed in a such way that the ratio of blubber thickness to body radius is nearly constant over the body (Ryg *et al*. 1988). Thermographic examination of harbour seals showed that the orbital, mystacial and supraorbital vibrissal pads are areas of excessive heat loss (Dehnhardt *et al*. 1998). Thermal imaging was not feasible in this study due to the endangered status of the Saimaa ringed seal.

We conclude that Saimaa and Baltic ringed seals corresponded to the pattern of large, complex maxilloturbinates (Van Valkenburgh *et al.* 2011) and the well-developed conchal mucosal and ophthalmic retia reported from many aquatic mammal species (Folkow *et al*. 1988, Ninomiya *et al*. 2014). Further studies with histological sections and 3D X-ray microcomputed tomography (Martinez *et al.* 2023) are needed to quantify the turbinal bone surface area in ringed seals. As the number of ringed seal skulls in museum collections is extensive, osteological analysis provides a potentially fruitful source for future comparative studies on pinniped maxilloturbinates (Mason *et al.* 2020).

Acknowledgements

It was a great pleasure to contribute to this celebratory volume for Professor Björn Kurtén, whose mind-broadening lectures two of us (JL, JJ) were privileged to attend as students. The Metsähallitus Seal Group collected the carcasses and provided background information on the specimens. DVM Marja Isomursu performed necropsies on some of the specimens in Oulu, allowing us to collect eye and other samples. We thank DVM Vilma Reunanen and the radiographers of the Veterinary Teaching Hospital of the University of Helsinki for expertly carrying out and optimizing the imaging of the selected ringed seals and providing technical information on the imaging methods used for this paper. Voitto Haukisalmi, Martti Hildén and Janne Granroth provided access to the osteological collections of the Finnish Museum of Natural History in Helsinki. JL received funding for this research from the University of Helsinki and the Raija and Ossi Tuuliainen Foundation. JJ was funded by the Jane and Aatos Erkko Foundation (4-2013 and 5-2017).

References

Amano, M, Hayano, A. & Miyazaki, N. 2002: Geographic variation in the skull of the ringed seal, *Pusa hispida*. — *Journal of Mammalogy* 83: 370–380.

Auttila, M., Kurkilahti, M., Niemi, M., Levänen, R., Sipilä, T., Isomursu, M., Koskela, J. & Kunnasranta, M. 2016: Morphometrics, body condition, and growth of the ringed seal (*Pusa hispida saimensis*) in Lake Saimaa: Implications for conservation. — *Marine Mammal Science* 32: 252–267.

Boyd, R. B. 1975: A gross and microscopic study of the respiratory anatomy of the Antarctic Weddell seal, *Leptonychotes weddelli*. — *Journal of Morphology* 147: 309–336.

Carlton, C. & McKean, T. 1977: The carotid and orbital retia of the pronghorn, deer and elk. — *Anatomical Record* 189: 91–108.

Cheon, H. L., Kjelstrup, S., Kizilova, N., Flekkøy, E. G., Mason, M. J. & Folkow, L. P. 2023: Structure-function relationships in the nasal cavity of Arctic and subtropical seals. — *Biophysical Journal* 122: 4686–4698.

Craven, B., Neuberger, T., Paterson, E. G., Webb, A. G., Josephson, E. M., Morrison, E. E. & Settles, G. S. 2007: Reconstruction and morphometric analysis of the nasal airway of the dog (*Canis familaris*) and implications regarding olfactory airflow. — *Anatomical Record* 290: 1325–1340.

Crompton, A. W., Owerkowicz, T., Bhullar, B.-A. S. & Musinky, C. 2017: Structure of the nasal region of non-mammalian cynodonts and mammaliaforms: speculations on the evolution of mammalian endothermy. — *Journal of Vertebrate Paleontology* 37, e1269116, https://doi.org/10.1080/02724634.2017.1269116.

Curtis, A. A. & Van Valkenburgh, B. 2014: Beyond the sniffer: frontal sinuses in Carnivora. — *Anatomical Record* 297: 2047–2064.

Curtis, A. A., Lai, G., Wei, F. & Van Valkenburgh, B. 2014: Repeated loss of frontal sinuses in arctoid carnivorans. — *Journal of Morphology* 276: 22–32.

Debey, L. B. & Pyenson, N. D. 2013: Osteological correlates and phylogenetic analysis of deep diving in living and extinct pinnipeds: what good are big eyes? — *Marine Mammal Science* 29: 48–83.

Dehnhardt, G., Mauck, B. & Hyvärinen, H. 1998: Ambient temperature does not affect the tactile sensitivity of mystical vibrissae in harbour seals. — *Journal of Experi-*

mental Biology 201: 3023–3029.

Dolezal, R. F. & Baker, R. S. 1983: Mucociliary flow in the canine frontal sinus. — *Annals of Otology, Rhinology & Laryngology* 92: 78–80.

Endo, H., Sasaki, H., Hayashi, Y., Petrov, E. A., Amano, M., Suzuki, N. & Miyazaki, N. 1999: CT examination of the head of the Baikal seal (*Phoca sibirica*). — *Journal of Anatomy* 194: 119–126.

Erdsack, N., Dehnhardt, G. & Hanke, W. 2014: Thermoregulation of the vibrissal system in harbour seals (*Phoca vitulina*) and Cape fur seals (*Arctocephalus pusillus pusillus*). — *Journal of Experimental Marine Biology and Ecology* 452: 111–118.

Flekkøy, E. G., Folkow, L. P., Kjelstrup, S., Mason, M. J. & Wilhelmsen, Ø. 2023: Thermal modeling of the respiratory turbinates in arctic and subtropical seals. — *Journal of Thermal Biology* 112, 103402, https://doi.org/10.1016/j.therbio.2022.103402.

Folkow, L. P. & Blix, A. S. 1987: Nasal heat and water exchange in gray seals. — *American Journal of Physiology* 253: R883–R889.

Folkow, L. P., Blix, A. S. & Eide, T. J. 1988: Anatomical and functional aspects of the nasal mucosal and ophthalmic retia of phocid seals. — *Journal of Zoology* 216: 417–436.

Granroth, J. & Laakkonen, J. 2023: Comparison of chemical and enzymatic maceration processes for soft tissue removal from arterial silicone casts on skull scaffolds. — *Anatomy, Histologia, Embryologia* 53, e12981, https://doi.org/10.1111/ahe.12981.

Green, P. A., Van Valkenburgh, B., Pang, B., Bird, D., Rowe, T. & Curtis, A. 2012: Respiratory and olfactory turbinal size in canid and arctoid carnivorans. — *Journal of Anatomy* 221: 609–621.

Hillenius, W. J. & Ruben, J. A. 2004: The evolution of endothermy in terrestrial vertebrates: who?, when?, why? — *Physiological and Biochemical Zoology* 77: 1019–1042.

Hillenius, W. J. 1992: The evolution of nasal turbinates and mammalian endothermy. — *Paleobiology* 18: 17–29.

Huntley, A. C., Costa, D. P. & Rubin, R. D. 1984: The contribution of nasal countercurrent heat exchange to water balance in the northern elephant seal, *Mirounga angustirostris*. — *Journal of Experimental Biology* 113: 447–454.

Hyvärinen, H. 1989: Diving in darkness — whiskers as sense organs of the ringed seal (*Phoca hispida saimensis*). — *Journal of Zoology* 218: 663–678.

Hyvärinen, H. & Katajisto, H. 1984: Functional structure of the vibrissae of the ringed seal (*Phoca hispida* Schr.). — *Acta Zoologica Fennica* 171: 27–30.

Hyvärinen, H. & Nieminen, M. 1990: Differentation of the ringed seal in the Baltic Sea, Lake Ladoga and Lake Saimaa. — *Finnish Game Research* 47: 21–27.

Irving, L. & Hart, J. S. 1957: The metabolism of seals as bare-skinned animals in cold water. –*Canadian Journal of Zoology* 35: 498–511.

Jackson, D. C. & Schmidt-Nielsen, K. 1964: Countercurrent heat exchange in the respiratory passages. — *Proceedings of the National Academy of Sciences USA* 51: 1192–1197.

Jamieson, G. S. & Fisher, D. 1972: The pinniped eye: a review. — In: Harrison, R. J. (ed.), *Functional anatomy of marine mammals*: 245–261. Academic Press, London.

Jones, K. E., Smaers, J. B. & Goswani, A. 2015: Impact of the terrestrial-aquatic transition on disparity and rates of evolution in the carnivoran skull. — *BMC Evolutionary Biology* 15, 8, https://doi.org/10.1186/s12862-015-0285-5.

Käkelä, R. & Hyvärinen, H. 1993: Fatty acid composition of fats around the mystical and superciliary vibrissae differs from that of blubber in the Saimaa ringed seal (*Phoca hispida saimensis*). — *Comparative Biochemistry and Physiology B* 105: 547–552.

Laakkonen, J. 2021: Distribution and morphology of ventricular bands in the hearts of ringed seals. — *Anatomia Histologia Embryologia* 50: 756–759.

Laakkonen, J. & Jernvall, J. 2016: Macroscopic anatomy of the Saimaa (*Phoca hispida saimensis*) lower respiratory tract. — *Anatomical Record* 299: 538–543.

Laakkonen, J. & Jernvall, J. 2020: The muscles of mastication and the temporo-mandibular joint of the Saimaa (*Pusa hispida saimensis*) and Baltic (*Pusa hispida botnica*) ringed seals. — *Annales Zoologici Fennici* 57: 21–29.

Laakkonen, J. & Kivalo, M. 2013: The use of silicone casts in collection of morphological data from free-ranging wildlife — the case of tracheobronchial anatomy of the Eurasian lynx (*Lynx lynx*). — *Annales Zoologici Fennici* 50: 256–261.

Laakkonen, J. & Nihtilä, H. 2021: Comparison of the musculoskeletal forelimb anatomy of the Saimaa (*Pusa hispida saimensis*) and Baltic (*Pusa hispida botnica*) ringed seals. — *Marine Mammal Science* 37: 1552–1563.

Laakkonen, J. & Vedrines, A. 2022: Hip and stifle joint anatomy of the Saimaa (*Pusa hispida saimensis*) and Baltic (*Pusa hispida botnica*) ringed seals. — *Anatomia Histologia Embryologia* 51: 314–317.

Laakkonen, J., Nihtilä, H. & Jernvall, J. 2024: Anatomical variations in the cerebral arterial circle of the Saimaa (*Pusa hispida saimensis*) and Baltic ringed seals (*Pusa hispida botnica*). — *The Anatomical Record* 307: 677–685.

Lester, C. W. & Costa, D. P. 2006: Water conservation in fasting northern elephant seals (*Mirounga angustirostgis*). — *Journal of Experimental Biology* 209: 4283–4294.

Ling, J. K. 1977: Vibrissae of marine mammals. — In: Harrison, R. J. (ed.), *Functional anatomy of marine mammals*: 387–415. Academic Press, London, New York, San Francisco.

Löytynoja, A., Rastas, P., Valtonen, M., Kammonen, J., Holm, L., Paulin, L., Jernvall, J. & Auvinen, P. 2023: Fragmented habitat compensates for the adverse effects of genetic bottleneck. — *Current Biology* 33: 1009–1018.

Macrini, T. E. 2012: Comparative morphology of the internal nasal skeleton of adult marsupials based on X-ray computed tomography. — *Bulletin of American museum of Natural History* 365: 1–91.

Martinez, Q., Okrouhlik, J., Šumbera, R., Wright, M., Araújo, R., Braude, S., Hildebrandt, T. B., Holtze, S., Ruf, I. & Fabre, P.-H. 2023: Mammalian maxilloturbinal evolution does not reflect thermal biology. — *Nature Communications* 14, 4425, https://doi.org/10.1038/s41467-

023-39994-1.

Mason, M. J., Wenger, L. M. D. & Hammer, Ø. & Blix, A. S. 2020: Structure and function of respiratory turbinates in phocid seals. — *Polar Biology* 43: 157–173.

Mass, A. M. & Supin, A. 2007: Adaptive features of aquatic mammals' eye. — *Anatomical Record* 290: 701–715.

Mills, R. P. & Christmas, H. E. 1990: Applied comparative anatomy of nasal turbinates. — *Clinical Otolaryngology* 15: 553–558.

Milne, A. O., Muchlinski, M. N., Orton, L. D., Sullivan, M. S. & Grant, R. A. 2022: Comparing vibrissal morphology and infraorbital foramen area in pinnipeds. — *Anatomical Record* 305: 556–567.

Moore, W. J. 1981: *The mammalian skull.* — Cambridge University Press, Cambridge, UK.

Murie, J. 1874: Researches upon the anatomia of pinnipedia. III. Descriptive anatomy of the sea-lion (*Otaria jubata*). — *Transactions of the Zoological Society of London* 8: 501–591.

Negus, V. E. 1958: *The comparative anatomy and physiology of the nose and paranasal sinuses.* — E. & S. Livingstone Ltd., Edinburgh.

Ninomiya, H. & Yoshida, E. 2007: Functional anatomy of the ocular circulatory system: vascular corrosion casts of the cetacean eye. — *Veterinary Ophthalmology* 10: 231–238.

Ninomiya, H., Imamura, E. & Inomata, T. 2014: Comparative anatomy of the ophthalmic rete and its relationship to ocular blood flow in three species of marine mammal. — *Veterinary Ophthalmology* 17: 100–105.

Ortiz, C. L., Costa, D. P. & Le Boeuf, B. J. 1978: Water and energy flux in fasting weaned elephant seal pups, *Mirounga angustirostris*. — *Physiological Zoology* 51: 166–178.

Owerkowicz, T., Musinsky, C., Middleton, K. M. & Crompton, A. W. 2015: Respiratory turbinates and the evolution of endothermy in mammals and birds. — In: Brainerd, E. L., Dial, K. & Shubin, N. H. (eds.), *The great transformations in vertebrate evolution*: 143–166. University of Chicago Press, Chicago.

Repenning, C. A. 1976: Adaptive evolution of sea lions and walruses. — *American Zoology* 25: 375–390.

Rowe, T., Eiting, T. P., Macrini, T. E. & Ketcham, R. A. 2005: Organization of the olfactory and respiratory skeleton in the nose of the gray short-tailed opossum *Monodelphis domestica*. — *Journal of Mammalian Evolution* 12: 303–336.

Ryg, M., Smith, T. G. & Øritsland, N. A. 1988: Thermal significance of the topographical distribution of blubber in ringed seals (*Phoca hispida*). — *Canadian Journal of Fisheries and Aquatic Sciences* 45: 985–992.

Schmidt-Nielsen, K., Hainsworth, F. R. & Murrish, D. E. 1970: Counter-current heat exchange in the respiratory passages: Effect on water and heat balance. — *Respiratory Physiology* 9: 263–276.

Scholander, P. F., Walters, V., Hock, R. & Irving, L. 1950: Body insulation of some arctic and tropical mammals and birds. — *Biological Bulletin* 99: 225–236.

Scott, J. H. 1954: Heat regulating function of the nasal mucous membrane. — *Journal of Laryngology & Otology* 68: 308–317.

Simoens, P., Muylle, S. & Lauwers, H. 1996: Anatomy of the ocular arteries in the horse. — *Equine Veterinary Journal* 28: 360–367.

Smith, T., Rossie, J. B. & Bhatnagar, K. 2007: Evolution of the nose and nasal skeleton in primates. — *Evolutionary Anthropology* 16: 132–146.

Smodlaka, H., Khamas, W. A., Palmer, L., Lui, B, Borovac, J. A., Cohn, B. A. & Schmitz, L. 2016: Eye histology and ganglion cell topography of northern elephant seals (*Mirounga angustirostris*). — *Anatomical Record* 299: 798–805.

Tandler, J. 1899: Zur vergleichenden anatomie der Kopfarterien bei den Mammalia. — *Denkschriften der Kaiserlichen Akademie der Wissenschaffen* 67: 677–783.

Usenius, T., Mustonen, A. M., Usenius, J. P., Hyvärinen, H., Sipilä, T., Koskela, J. T. & Nieminen, P. 2007: Magnetic resonance imaging and its applications in morphological studies of pinnipeds. — *Annales Zoologici Fennici* 44: 355–367.

Van Valkenburgh, B., Smith, T. D. & Craven, B. A. 2014a: Tour of a labyrinth: exploring the vertebrate nose. – *Anatomical Record* 297: 1975–1984.

Van Valkenburgh, B., Curtis, A., Samuels, J. X., Bird, D., Fulkerson, B., Meachen-Samuels, J. & Slater, G. J. 2011: Aquatic adaptations in the nose of carnivorans: evidence from the turbinates. — *Journal of Anatomy* 218: 298–310.

Van Valkenburgh, B., Pang, B., Bird, D., Curtis, A., Yee, K., Wysocki, C. & Craven, B. A. 2014b: Respiratory and olfactory turbinals in filiform and caniform carnivorans: the influence of snout length. — *Anatomical Record* 297: 2065–2079.

Walker, J. E. C. & Wells, R. E. 1961: Heat and water exchange in the respiratory tract. — *The American Journal of Medicine* 30: 259–267.

Welsch, U., Ramdohr, S., Riedelsheimer, B., Hebel, R., Eisert, R. & Plötz, J. 2001: Microscopic anatomy of the eye of the deep-diving Antarctic Weddell seal (*Leptonychotes weddellii*). — *Journal of Morphology* 248: 165–174.

Witmer, L. M. 1997: The evolution of the ant orbital cavity of archosaurs: a study in soft tissue reconstruction in the fossil record with an analysis of the function of pneumaticity. — *Journal of Vertebrate Paleontology* 17: 1–17, https://doi.org/10.1080/02724634.1997.10011027.